

Uncertainty Quantification in SVM prediction

Pritam Anand
DA-IICT, Gandhinagar.

pritam_anand@daiict.ac.in

Abstract

This paper explores Uncertainty Quantification (UQ) in SVM predictions, particularly for regression and forecasting tasks. Unlike the Neural Network, the SVM solutions are typically more stable, sparse, optimal and interpretable. However, there are only few literature which addresses the UQ in SVM prediction. At first, we provide a comprehensive summary of existing Prediction Interval (PI) estimation and probabilistic forecasting methods developed in the SVM framework and evaluate them against the key properties expected from an ideal PI model. We find that none of the existing SVM PI models achieves a sparse solution, which has remained a key advantage of the standard SVM model developed for classification and regression tasks. To introduce sparsity in SVM model, we propose the Sparse Support Vector Quantile Regression (SSVQR) model, which constructs PIs and probabilistic forecasts by solving a pair of linear programs. Further, we develop a feature selection algorithm for PI estimation using SSVQR that effectively eliminates a significant number of features while improving PI quality in case of high-dimensional dataset. Finally we extend the SVM models in Conformal Regression setting for obtaining more stable prediction set with finite test set guarantees. Extensive experiments on artificial, real-world benchmark datasets compare the different characteristics of both existing and proposed SVM-based PI estimation methods and also highlight the advantages of the feature selection in PI estimation. Furthermore, we compare both, the existing and proposed SVM-based PI estimation models, with modern deep learning models for probabilistic forecasting tasks on benchmark datasets. Furthermore, SVM models show comparable or superior performance to modern complex deep learning models for probabilistic forecasting task in our experiments. The code are available at <https://github.com/ltpritamanand/-PI-IN-SVM->.

1 Introduction

Given the training set $T = \{(x_i, y_i) : x_i \in \mathbf{R}^n, y_i \in \mathbf{R}, i = 1, 2, \dots, m\}$, sampled independently from the joint distribution of the random variables (X, Y) , the goal of the regression task is to estimate a function that predicts the target variable y based on the input variable x well. However, in most of applications, the prediction of the regression model may not be perfectly accurate due to random relationship between Y and X . For example, predicting the impact of a specific drug on a patient's heart rate based on their Body Mass Index (BMI) may not be accurate and may involve a significant degree of uncertainty. In such cases, quantifying these uncertainties is crucial for making effective decisions.

The Prediction Interval (PI) estimation is most commonly used Uncertainty Quantification (UQ) technique in regression tasks. Given a high confidence $1 - \alpha \in (0, 1)$ and training set T , the PI tube is defined as a pair of functions (f_1, f_2) . It is said to be well calibrated if it satisfies $P(f_1(X) \leq Y \leq f_2(X) | X) \geq 1 - \alpha$. The objective of the PI models is to obtain a PI tube with the minimum possible width while ensuring the target calibration. Therefore, the performance of a PI estimation method is mainly evaluated using two criteria: Prediction Interval Coverage Probability (PICP), which computes the fraction of y values within the PI tube, and Mean Prediction Interval Width (MPIW), quantifying the width of the PI tube.

The PI estimation models requires to explore the different characteristics of the conditional distribution $Y|X$, rather focusing only on $E(Y|X)$ as done in standard regression tasks. The basic approach of PI models involves estimating a pair of quantile functions (Koenker & Bassett Jr (1978)), say $(f_q(x), f_{1+q-\alpha}(x))$, of the

conditional distribution $Y|X$, for some $0 \leq q \leq \alpha$, where the q^{th} quantile function for given x is defined as infimum of functions satisfying $P(y \leq f_q(x)|x) = q$.

For time-series data, estimating the Prediction Interval (PI) for future observations using an auto-regressive approach is referred to as probabilistic forecasting. Both PI estimation and probabilistic forecasting models are widely investigated in the Neural Network (NN) architectures in the literature. The PI estimation methods in the NN literature can primarily be divided into two main categories. A popular class of PI estimation methods assumes that the conditional distribution $Y|X$ follows a particular distribution (often normal) and obtains the quantile functions by computing the inverse of the corresponding cumulative distribution function. Some important of them are Bayesian method (MacKay (1992); Bishop (1995), Delta method De VIEAUX et al. (1998); Hwang & Ding (1997); Seber & Seber (2015)) and Mean Variation Estimation (MVE) method (Nix & Weigend (1994)). Some of the recent NN architecture for the probabilistic forecasting task with distribution assumptions are Mix Density Network (Bishop (1994); Zhang et al. (2020a)), Deep Auto-regressive Network (Deep AR) (Salinas et al. (2020)).

The other class of PI estimation and probabilistic forecasting methods believe in estimating the pair of quantile functions $(f_q(x), f_{1+q-\alpha}(x))$ in distribution-free setting without imposing any assumption regarding the distribution of $Y|X$. For estimation of the q^{th} quantile function, $f_q(x)$, most of them minimize the pinball loss function. The pinball loss-based NN model, also known as Quantile Regression Neural Network (QRNN) (Taylor (2000); Cannon (2011)) is the main PI estimation method, which has been utilized in various engineering applications. The pinball loss-based NN model has been frequently applied to probabilistic forecasting of wind (Wan et al. (2016)), electric load (Zhang et al. (2018; 2020b)), electric consumption (He et al. (2019)), flood risks (Pasche & Engelke (2024)) and solar energy (Lauret et al. (2017)). Some of the distribution-free PI estimation NN methods consider the minimization of a particularly designed loss function for the direct and simultaneous estimation of the bounds of the PI. Some of them are Lower Upper Bound Estimation (LUBE) NN, Quality-Driven (QD) Loss NN (Pearce et al. (2018)) and Tube loss NN (Anand et al. (2024)).

However, a well-calibrated HQ PI guarantees the target coverage level t only asymptotically, and may fail to achieve it on finite test samples. In real-world decision-making, especially in high-stakes applications, guarantees on finite test samples coverage are often essential. Conformal Regression (CR) (Vovk et al. (1999; 2005)) provides a principled framework through which PI models can be adapted to ensure such finite-sample coverage guarantees, making them more suitable for practical deployment.

Despite the remarkable success of neural architectures, researchers still prefer SVMs for their predictive accuracy in regression tasks, particularly when dealing with small size tabular dataset. This is because SVM regression models explicitly incorporate regularization and most of them minimize a convex program to guarantee a global optimal, interpretable and sparse solutions, which remain missing in the NN learning.

Compared to SVM models, NN and deep learning-based regression models typically exhibit a higher degree of model uncertainty. This arises for two main reasons. First, neural models generally have a much larger number of parameters than SVMs, making them more prone to variability. Second, due to the non-convex nature of their optimization landscape, NN models often converge to different local minima across different training trails, even under identical training set and hyperparameter settings.

However, in contrast to NN literature, there are only a few SVM methods which target the PI estimation and probabilistic forecasting tasks in the literature. Moreover, SVM models have been largely unexplored within conformal regression setting. Our work addresses these gaps in the literature by extending contemporary UQ techniques to the SVM framework, supported by a comprehensive analysis and comparisons. We summarize the contribution of our work in detail as follows.

- (a) First, we carefully review the existing literature on PI estimation and probabilistic forecasting methods in SVM. We outline the desirable properties of an ideal PI model and compare the PI estimation and probabilistic forecasting methods in SVM against them. We find that only two of SVM PI methods attain the global optimal solution but, none of them achieve a sparse solution vector.
- (b) Building on this motivation, we propose a sparse SVM method for Prediction Interval (PI) estimation and probabilistic forecasting. Our Sparse SVM model enhances the PI estimation process by reducing

the overall complexity of learning and prediction while preserving the classical properties of SVM, achieving both a globally optimal and sparse solution. Further, we highlight the importance of the feature selection in PI estimation particularly in high dimensional regression tasks. For this, we develop a simple yet effective feature selection algorithm for PI estimation using our sparse SVM PI model. We show that our algorithm does not only successfully discard a significant percentage of features but, also improves the quality of the PI while learning the PI for high-dimensional data. To the best of our knowledge, there is no any existing literature which study the feature selection problem in context of PI estimation.

- (c) Finally, we extend SVM regression to the conformal regression setting to achieve finite-sample coverage guarantees. Compared to NN, we show that the conformal prediction sets produced by SVM models are more stable and interpretable due to its global optimal solution.
- (d) We conduct extensive experiments on artificial, real-world benchmark datasets to empirically analyze the PI quality obtained by the both existing and proposed PI estimation models in SVM. For high-dimensional datasets, we reveal the effectiveness of the Sparse SVM-based PI model by performing feature selection using sparse SVM PI based feature selection algorithm. Our numerical result also demonstrate that the SVM based probabilistic forecasting models can achieve comparable, and in some cases superior, PI quality relative to recent complex deep probabilistic forecasting models that involve significantly larger numbers of parameters on few benchmark datasets.

The remainder of this paper is structured as follows. Section 2 provides a systematic review of the prerequisite concepts required for understanding of the SVM models and UQ techniques. Section-3 provides a detail description of the several SVM models for PI estimation and probabilistic forecasting, highlighting their advantages and limitations. In Section 4, we introduce the proposed Sparse SVM models for PI estimation, probabilistic forecasting and conformal regression tasks. Section 5 presents the numerical results from extensive experiments, demonstrating the effectiveness of the proposed SVM model for PI estimation and probabilistic forecasting tasks. Section 6 outlines the future work.

2 Related key concepts

In this section, we will outline key concepts and methods relevant to PI estimation techniques in SVM.

2.1 Quantile Regression and SVM

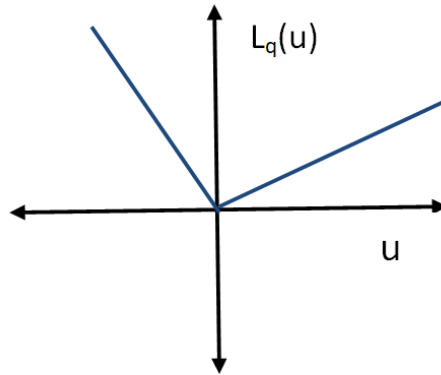


Figure 1: Pinball loss function

In distribution free setting, for a given quantile $q \in (0, 1)$, the quantile value is estimated by minimizing the pinball loss function, which is given by

$$\rho_q(u) = \begin{cases} qu, & \text{if } u \geq 0, \\ (q-1)u, & \text{Otherwise,} \end{cases} \quad (1)$$

For the estimation of the conditional quantile function, u represents the error obtained by the subtracting the estimates $f(x_i)$ from its target values y_i . For a given quantile $q \in (0, 1)$, training set $T = \{(x_i, y_i) : x_i \in \mathbf{R}^n, y_i \in \mathbf{R}, i = 1, 2, \dots, m\}$ and class of function F , let us suppose that f_T is the solution of the problem $\min_{f \in F} \sum_{i=1}^m \rho_q(y - f(x_i))$. Takeuchi et al., have shown that the fraction of y values lying below the function $f_T(x)$ is bounded from above by qm and asymptotically equals qm with probability 1 under a very general condition in their work (Takeuchi et al. (2006)).

Given the training set, SVM models estimate the function in the form of $f(x) = w^T \phi(x) + b$, where ϕ maps the input variable x into the high dimensional feature space, such that for any pair of x_i and x_j in \mathbf{R}^n , $\phi(x_i)^T \phi(x_j)$ can be obtained by the well defined kernel function $k(x_i, x_j)$. By the use of the kernel trick and representer theorem Schölkopf et al. (2001), the SVM estimate $f(x) = w^T \phi(x) + b$ can be represented by the kernel generated function in the form of $\sum_{i=1}^m k(x_i, x) u_i + b$, where k is positive-semi definite kernel Mercer (1909). This representation eliminates the need for explicit knowledge of the mapping ϕ .

2.2 Support Vector Quantile Regression model

The Support Vector Quantile Regression (SVQR) model minimizes the L_2 -norm of the regularization along with the empirical risk computed by the pinball loss function. For q^{th} quantile function estimation, it seeks the solution of the problem

$$\min_{(w,b)} \frac{1}{2} w^T w + C \sum_{i=1}^m \rho_q(y_i - (w^T \phi(x_i) + b)), \quad (2)$$

which can be equivalently converted to the following Quadratic Programming Problem (QPP)

$$\begin{aligned} & \min_{(w,b,\xi,\xi^*)} \frac{1}{2} w^T w + C \sum_{i=1}^m (q\xi_i + (1-q)\xi_i^*) \\ & \text{subject to,} \\ & y_i - (w^T \phi(x_i) + b) \leq \xi_i, \\ & (w^T \phi(x_i) + b) - y_i \leq \xi_i^*, \\ & \xi_i, \xi_i^* \geq 0, \quad i = 1, 2, \dots, m, \end{aligned} \quad (3)$$

where $C \geq 0$ is the user defined parameter for trading-off the empirical risk against the model complexity.

To efficiently solve QPP (3), we often focus on obtaining the solution to its corresponding Wolfe dual problem, which is given by

$$\begin{aligned} & \min_{(\alpha,\beta)} \sum_{i=1}^m \sum_{j=1}^m (\alpha_i - \beta_i) k(x_i, x_j) (\alpha_j - \beta_j) - \sum_{i=1}^m (\alpha_i - \beta_i) y_i \\ & \text{subject to,} \\ & \sum_{i=1}^m (\alpha_i - \beta_i) = 0, \\ & 0 \leq \alpha_i \leq Cq, \quad i = 1, 2, \dots, m, \\ & 0 \leq \beta_i \leq C(1-q), \quad i = 1, 2, \dots, m, \end{aligned} \quad (4)$$

where $(\alpha_i, \beta_i), i = 1, 2, \dots, m$, are Lagrangian multipliers.

After obtaining the optimal solution of the dual problem (4), $(\alpha_i^*, \beta_i^*), i = 1, 2, \dots, m$, the q^{th} quantile function is estimated by

$$f_q(x) = \sum_{i=1}^m (\alpha_i^* - \beta_i^*) k(x_i, x) + b. \quad (5)$$

The estimation of the bias term b can be obtained by using the KKT conditions of the primal problem (3). For this, we need to select the every training point (x_k, y_k) which corresponds to $0 < \alpha_k^* < Cq$ or

$0 < \beta_k^* < C(1 - q)$ and compute

$$b_k = y_k - \sum_{i=1}^m (\alpha_i^* - \beta_i^*) k(x_i, x_k). \quad (6)$$

The final value of bias b can be obtained by computing the mean of all b_k .

2.3 Least Squares Support Vector Regression

For estimating the mean regression using training set T , the LS-SVR model Suykens et al. (2002) minimizes the least square loss function along with the L_2 -norm of regularization in the following problem.

$$\begin{aligned} \min_{(w, b, \xi)} \quad & \frac{1}{2} w^T w + C \sum_{i=1}^m (\xi_i^2) \\ \text{subject to,} \quad & y_i - (w^T \phi(x) + b) = \xi_i, \quad i = 1, 2, \dots, m. \end{aligned} \quad (7)$$

The solution of problem (7) can be obtained through the following system of equations

$$\begin{bmatrix} 0 & e^T \\ e & K(A, A^T) + \frac{2}{C} I \end{bmatrix} \begin{bmatrix} b \\ \alpha \end{bmatrix} = \begin{bmatrix} 0 \\ Y \end{bmatrix}, \quad (8)$$

where $K(A, A^T)$ is an $m \times m$ kernel matrix constructed from the training set T , e is an m -dimensional column vector of ones, and I represents the $m \times m$ identity matrix. After obtaining the (b, α) from (8), the LS-SVR estimates the regression function for a given $x \in \mathbb{R}^n$ using

$$f(x) = \sum_{i=1}^m k(x_i, x) \alpha_i + b. \quad (9)$$

2.4 Probabilistic Forecasting

The task of probabilistic forecasting is basically an extension of the PI estimation in an auto-regressive setting. Consider the time series observations $T = \{x_1, x_2, \dots, x_t\}$, recorded on t different time stamps. If $p < t$ denotes the effective lag window, then auto-regressive models estimate the relationship between $z_i := (x_{i-p+1}, \dots, x_i)$ and x_{i+1} for $i = p, p+1, \dots, t-1$ using the training set T , and use this learned relationship to forecast future observations. Point forecasting models aim to estimate the conditional expectation $E(x_{i+1} | z_i)$. However, in many cases, such forecasts may incur significant errors due to inherent noise and volatility in the data. Probabilistic forecasting quantifies these uncertainties in the prediction by obtaining the PI.

The task of probabilistic forecasting is to estimate the PI for x_{i+1} given the input z_i for $i \geq t$. The SVM based probabilistic forecasting models obtain the estimate of the PI $[\hat{F}_q(z_i), \hat{F}_{1+q-\alpha}(z_i)]$, where $\hat{F}_q(z_i)$ and $\hat{F}_{1+q-\alpha}(z_i)$ are kernel generated functions, estimating of the q^{th} and $(1 - \alpha - q)^{th}$ quantiles of the conditional distribution $(x_{i+1} | z_i)$ for some $q \in (0, \alpha)$. Distribution-free probabilistic forecasting methods estimate quantile functions directly, without making any assumptions about the conditional distribution $(x_{i+1} | z_i)$.

2.5 Conformal Regression

Conformal Regression (Vovk et al. (1999; 2005)) provides a general framework for adjusting PI models to guarantee the target coverage $1 - \alpha$ on finite test samples, assuming only that the data are exchangeable.

The split conformal regression (CR) approach (Papadopoulos et al. (2002); Papadopoulos (2008)) starts by dividing the available training data T into two separate subsets: a training set I_1 used to fit the predictive model, and a calibration set I_2 used for PI adjustment. A nonconformity score function is then introduced to quantify the disagreement between predicted value for y_i , given input x_i and its actual observed value. These nonconformity scores are computed on the calibration set I_2 . A obvious choice of the non-conformity

score is the absolute residual value, computed by $|y_i - \hat{f}(x_i)|$, $i \in I_2$, where \hat{f} is the estimate of the mean regression model trained on I_1 .

Romano et al. have developed the quantile regression based nonconformity score for obtaining the fully adaptive conformal prediction set in their work Conformalized Quantile Regression (CQR) (Romano et al. (2019)), which is given by

$$E_i = \max\{\hat{F}_{lo}(x) - y_i, y_i - \hat{F}_{hi}(x)\}, \quad (10)$$

where $\hat{F}_{lo}(x)$ and $\hat{F}_{hi}(x)$ are the estimates of the q^{th} and $(1 + q - \alpha)^{th}$ quantile function on set I_1 for some $0 \leq q \leq \alpha$.

After computing the non-conformity scores, the CR methodology requires the computation of $(1 - \alpha)(1 + \frac{1}{|I_2|})$ -th empirical quantile of the non-conformity score. In case of CQR, we denote it with $Q_{1-\alpha}(E_i, I_2)$ and obtain the prediction set on new test point x_{m+1} as

$$C(x_{m+1}) = [\hat{F}_{lo}(x_{m+1}) - Q_{(1-\alpha)}(E, I_2), \hat{F}_{hi}(x_{m+1}) + Q_{1-\alpha}(E, I_2)] \quad (11)$$

3 PI estimation in SVM

In this section, we gather in detail the PI estimation and probabilistic forecasting methods developed in the SVM literature and compare their advantages and limitations.

3.1 PI estimation through LS-SVR

One of the naive PI estimation method in SVM literature follows the normal assumption regarding the distribution of $Y|X$ and estimate its mean through (9) by training the LS-SVR model. The error distribution $\epsilon_i = y_i - f(x_i)$ follows a normal distribution with a mean of zero and variance σ . This variance can be estimated from the error computed on training set T . The pair of quantile bounds required for PI is estimated as $(f(\hat{x}) + \epsilon_{\frac{\alpha}{2}}, f(\hat{x}) + \epsilon_{1-\frac{\alpha}{2}})$, where ϵ_q is the q^{th} quantile of the error. A more refined and bias-corrected PI based on the LS-SVR model is proposed in (De Brabanter et al. (2010); Cheng et al. (2014)).

3.2 PI estimation through SVQR

Given the high confidence $1 - \alpha$ with training set T , the PI model requires the estimation of the pair of quantile functions $(f_q(x), f_{1+q-\alpha}(x))$ of the conditional distribution $Y|X$. The SVQR model can be trained twice for the estimation of the pair of these quantile functions for some $0 \leq q \leq \alpha$. We detail the algorithm for PI estimation through SVQR in Algorithm 1. At Algorithm 1, the tuning of C refers to selecting the value of C from a specified range such that the SVQR estimate obtains the least coverage error.

Algorithm 1 PI estimation through SVQR

- 1: **procedure** :- PI THROUGH SVQR($T, 1 - \alpha$)
 - 2: Choose some $\bar{q} \in (0, 1 - \alpha)$
 - 3: **for** each $q \in \{\bar{q}, (1 + \bar{q} - \alpha)\}$ **do**
 - 4: Solve the QPP problem (4) by tuning the value of C . Obtain the solution (α^*, β^*) .
 - 5: Estimate the function $f_q(x)$ using the (5).
 - 6: **return** $(f_{\bar{q}}(x), f_{1+\bar{q}-\alpha}(x))$
-

A key challenge in estimating prediction intervals (PI) using the quantile approach is to determine the good choice of \bar{q} for obtaining the narrower PI. For a symmetric noise distribution, $\bar{q} = \frac{\alpha}{2}$ is expected to produce the PI with minimum width. However, this does not hold for an asymmetric noise distribution. In the latter case, \bar{q} should be selected such that the resulting PI passes through the denser regions of the data cloud. Furthermore, for each choice of \bar{q} , the optimization problem (4) must be solved twice for $q = \bar{q}$ and $q = 1 + \bar{q} - \alpha$ to obtain the prediction interval (PI). It increases the overall computational complexity of the PI estimation process, making it both time-consuming and challenging in practice.

To simplify the PI estimation process, researchers have developed direct PI estimation methods, which solve a single optimization problem to obtain the both bounds of PI simultaneously. These methods are designed with a specialized loss function that can be minimized to obtain the both bounds of PI simultaneously. Some important of them are LUBE loss (Khosravi et al. (2010)), Quality-Driven (QD) loss (Pearce et al. (2018)) and Tube loss (Anand et al. (2024)) functions. We describe those also formulated within the SVM framework as follows.

3.3 PI estimation through Tube loss

(Anand et al. (2024)) have developed the Tube loss for PI estimation and probabilistic forecasting. It can be minimized directly to obtain the bounds of the PI simultaneously. The minimizer of the Tube loss function also guarantees the target coverage $1 - \alpha$ asymptotically. Also, the PI tube can also be shifted up or down by tuning its parameter r so that it can cross through the denser region of data cloud for minimal PI width. Furthermore, the width of the PI tube can be explicitly minimized in its optimization problem through the parameter δ . It helps to improve the PI width, when the PI tube achieves a coverage higher than the target on the validation set.

The Tube loss function is a kind of two-dimensional extension of the pinball loss function (Koenker & Bassett Jr (1978)). For a given $1 - \alpha \in (0, 1)$ and $u_2 \leq u_1$, the Tube loss function is given by

$$\rho_{1-\alpha}^r(u_2, u_1) = \begin{cases} (1 - \alpha)u_2, & \text{if } u_2 > 0, \\ -\alpha u_2, & \text{if } u_2 \leq 0, u_1 \geq 0 \text{ and } ru_2 + (1 - r)u_1 \geq 0, \\ \alpha u_1, & \text{if } u_2 \leq 0, u_1 \geq 0 \text{ and } ru_2 + (1 - r)u_1 < 0, \\ -(1 - \alpha)u_1, & \text{if } u_1 < 0, \end{cases} \quad (12)$$

where $0 < r < 1$ is a user-defined parameter and (u_2, u_1) are errors, representing the deviations of y values from the bounds of PI.

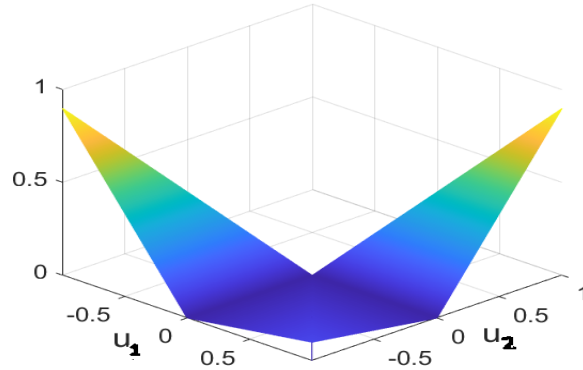


Figure 2: Tube loss function for $1 - \alpha = 0.9$.

Figure 2 illustrates the Tube loss for $(1 - \alpha) = 0.9$ with $r = 0.5$. For $r = 0.5$, the Tube loss function is always a continuous loss function of u_1 and u_2 , symmetrically positioned around the line $u_1 + u_2 = 0$. In all experiments with a symmetric noise distribution, the r parameter in the Tube loss function should be set to 0.5 to capture the denser region of y values.

The Tube loss SVM model seeks a pair of kernel generated functions

$$\mu_1(x) = \sum_{i=1}^m k(x_i, x)\alpha_i + b_1 \quad \text{and} \quad \mu_2(x) = \sum_{i=1}^m k(x_i, x)\beta_i + b_2 \quad (13)$$

by minimizing the optimization problem

| | LS-SVR PI | SVQR PI | LUBE | Tube loss |
|--------------------------|------------------------|---------|------|-----------|
| Distribution-free method | No | Yes | Yes | Yes |
| Asymptotic guarantees | Only with normal noise | Yes | No | Yes |
| Direct PI estimation | Yes | No | Yes | Yes |
| PI tube movement | No | Yes | No | Yes |
| Global optimal solution | Yes | Yes | No | No |
| Re-calibration | No | No | Yes | Yes |
| Sparsity | No | No | No | No |

Table 1: Comparisons of the Quantile , LUBE, QD loss and Tube loss based PI estimation models

$$\begin{aligned}
\min_{(\alpha, \beta, b_1, b_2)} J(\alpha, \beta, b_1, b_2) &= \frac{\lambda}{2} (\alpha^T \alpha + \beta^T \beta) + \sum_{i=1}^m \rho_{1-\alpha}^T(y_i, (K(A^T, x_i)\alpha + b_1), (K(A^T, x_i)\beta + b_2)) \\
&+ \delta \sum_{i=1}^m |(K(A^T, x_i)(\alpha - \beta) + (b_1 - b_2))|,
\end{aligned} \tag{14}$$

where δ, r and λ are user-defined parameters and A is the $m \times n$ data matrix containing the training set. Further, details on the Tube SVM problem and its minimization using gradient descent method can be found in (Anand et al. (2024)).

3.4 PI estimation through LUBE loss

The LUBE method (Khosravi et al. (2010)) was originally developed in the NN framework but, was extended in the SVM framework later in (Shrivastava et al. (2014; 2015)) for probabilistic forecasting of electric price. For the given target confidence $(1 - \alpha)$, and training set T , the LUBE SVM model seeks a pair of kernel generated functions of 13, $\mu_1(x)$ and $\mu_2(x)$, which are obtained by minimizing the following loss function

$$CWC = \frac{1}{R} MPIW (1 + \gamma (PICP) e^{-\eta (PICP - (1-\alpha))}). \tag{15}$$

Here, MPIW is the average width of estimated PI on training set, computed by $\frac{1}{m} \sum_{i=1}^m (\mu_2(x_i) - \mu_1(x_i))$. As discussed earlier, the PICP is the coverage of the estimated PI and computed using the $PICP = \frac{1}{m} \sum_{i=1}^m k_i$, where

$$k_i = \begin{cases} 1, & \text{if } y_i \in [\mu_1(x), \mu_2(x)]. \\ 0, & \text{Otherwise.} \end{cases}$$

Further, the $\gamma(PICP) = \begin{cases} 0, & \text{if } PICP \geq 1 - \alpha, \\ 1, & \text{otherwise,} \end{cases}$, R is the range of response values y_i and η is the user-defined parameter.

The major problem with the LUBE cost function (15) is that it is very difficult to be optimized because, the PICP is a step function. Khosravi et al. have solved the LUBE cost function (15) using the Particle Swarm Optimization (PSO) (Kennedy & Eberhart (1995)) to estimate the PI. However, due to sub-optimal solution, high-quality PI is not always observed. Pearce et al. refine the LUBE cost function and use a sigmoidal function to approximate the PICP, allowing the application of the gradient descent method for training the NN for PI estimating in their work (Pearce et al. (2018)).

3.5 Comparison of PI estimation SVM models

In Table 1, we visualize the desirable properties for a PI estimation model and compare the SVM methods in light of them with a detailed discussion as follows.

-
- (a) Distribution-free method : - The LS-SVR PI model assumes that the underlying noise distribution of the data is normal and may obtain poor estimate otherwise. In the literature, distribution-based PI methods often struggle to achieve consistent performance across various datasets. The SVQR, LUBE, and Tube loss methods provide PI estimation without assuming any specific distribution, allowing them to generate high-quality PI even in the presence of non-normal noise.
 - (b) Asymptotic guarantees:- A fundamental requirement in PI estimation models is that the obtained PI should guarantee the target coverage $1 - \alpha$ at least asymptotically, which remain missing in the LUBE method. The LS-SVR PI model provides this guarantee only in presence of normal noise. The SVQR and Tube loss based PI methods provide this asymptotic guarantee.
 - (c) Direct PI estimation:- As detailed in Algorithm 1, the SVQR PI model obtains the two bounds of PI by solving pair of SVQR problems one by one. The LUBE and Tube loss-based PI models simultaneously obtain the bounds of the PI by solving a single optimization problem.
 - (d) PI tube movement:- The PI tube movement is one another important desirable feature for PI estimation. This movement allows the PI to pass through the denser regions of the data cloud, helping to minimize the width of the PI, while achieving the target coverage. The centered PI is ideal only in the presence of the symmetric noise. However, in the presence of asymmetric noise in the data, the width of the prediction interval (PI) can be reduced by shifting it upward or downward without compromising its coverage. The SVQR and Tube loss-based PI models enable PI movement through their parameter \hat{q} and r respectively.
 - (e) Global Optimal Solution:- One of the attractive feature of the standard SVM methods is that they guarantee a global optimal solution by solving a convex optimization problem. However, in PI estimation, only the SVQR and LS-SVR based PI model maintains this guarantee by minimizing the convex loss function in its optimization problems. The Tube loss problem (14) is non-convex and hence fails to guarantee the global optimal solution. Furthermore, the LUBE problem (15) is highly discontinuous and relies on meta-heuristic algorithms for its solution. It often makes the LUBE solution suboptimal, resulting in poor PI quality.
 - (f) Re-calibration:- As detailed in Algorithm 1, the SVQR PI model obtains the bound of PI by solving the pair of SVQR problems one-by one. It can not explicitly minimize the width of PI in its optimization problem. This limitation prevents SVQR PI from using the recalibration feature. In recalibration, PI models are retrained to reduce interval width, when empirical coverage obtained on validation set exceeds the target $1 - \alpha$ significantly. During retraining, the PI models increases the value of the parameter (δ in case of the Tube loss) that trade-off the width of the PI against the coverage in the optimization problem. The LUBE and Tube loss-based models explicitly incorporate the minimization of prediction interval (PI) width in their problems, thereby enabling recalibration, which is practically useful for further reducing the PI width.
 - (g) Sparsity:- Sparsity is yet another promising feature offered by the initial SVM models developed for the classification and regression. However, it remains missing with all PI estimation models developed in the SVM framework.

4 Sparse PI estimation in SVM

In this section, we introduce the Sparse Support Vector Quantile Regression (SSVQR) model and detail the algorithm for obtaining the sparse PI through it. The SSVQR PI model inherits all properties of SVQR listed in Table 1 and also brings the sparse solution as well. Additionally, it addresses the feature selection problem in PI estimation efficiently and also obtain the sparse estimates in CR setting.

In literature, there are few works that obtain the sparse solution while minimizing the pinball loss function or its variants. Some of the literature such as (Taylor (2000); Rastogi et al. (2018)) obtains the sparse solution for the classification task in the SVM framework while minimizing the variant of the pinball loss function. In (Tanveer et al. (2021)), authors have obtained the sparse solution by minimizing a variant of the pinball

loss for clustering problem. For quantile estimation, there are a few literature like (Anand et al. (2020); Ye et al. (2025)) which attempt to develop the ϵ -insensitive variant of the pinball loss function, inspired by the ϵ -insensitive loss function used in standard SVM regression (Vapnik (2013)).

In view of the above literature, this paper propose a method for obtaining sparse PI estimates in the SVM by formulating the pinball loss minimization problem with L_1 -norm regularization as a linear programming problem (LPP) and further extends it to address the feature selection problem in PI estimation.

4.1 Sparse Support Vector Quantile Regression model

The SSVQR minimizes the pinball loss function with L_1 - norm regularization. It seeks the solution of the following problem

$$\min_{(w,b)} \frac{1}{2} \|w\|_1 + C \sum_{i=1}^m \rho_q(y_i - (w^T \phi(x_i) + b)), \quad (16)$$

where $C \geq 0$ is the user defined parameter for trading of the regularization against the empirical loss. The solution to problem (16) is sparse, similar to LASSO regression, as the minimization of the L_1 -norm regularization compels the weight coefficients to shrink to zero.

With the help of the kernel trick, the representor theorem rewrites the estimated function $f(x) = (w^T \phi(x) + b)$ as $\sum_{j=1}^m k(x_j, x) u_j + b$. It makes the SSVQR problem (16) equivalent to

$$\begin{aligned} & \min_{(u,b,\xi,\xi^*)} \frac{1}{2} \|u\|_1 + C \sum_{i=1}^m (q\xi_i + (1-q)\xi_i^*) \\ & \text{subject to,} \\ & y_i - \left(\sum_{j=1}^m k(x_j, x_i) u_j + b \right) \leq \xi_i, \\ & \left(\sum_{j=1}^m k(x_j, x_i) u_j + b \right) - y_i \leq \xi_i^*, \\ & \xi_i, \xi_i^* \geq 0, \quad i = 1, 2, \dots, m, \end{aligned} \quad (17)$$

Without loss of generality, let us consider the solution vector $u = r - p$, where r and p are vectors of positive numbers i.e., $r_i, p_i > 0, i = 1, 2, \dots, m$, then the problem (17) can be expressed as

$$\begin{aligned} & \min_{(r,p,b,\xi,\xi^*)} \frac{1}{2} \sum_{i=1}^m (r_i + p_i) + C \sum_{i=1}^m (q\xi_i + (1-q)\xi_i^*) \\ & \text{subject to,} \\ & y_i - \left(\sum_{j=1}^m k(x_j, x_i) (r_j - p_j) + b \right) \leq \xi_i, \\ & \left(\sum_{j=1}^m k(x_j, x_i) (r_j - p_j) + b \right) - y_i \leq \xi_i^*, \\ & \xi_i, \xi_i^*, r_i, p_i \geq 0, \quad i = 1, 2, \dots, m. \end{aligned} \quad (18)$$

The above problem (18) is a LPP with $4m$ variables, $2m$ linear constraints and $4m$ non-negative constraints, which can be efficiently solved by any LPP solver. The optimal solution (r^*, p^*, b^*) of the LPP (18) determines the estimate of the q^{th} quantile function using

$$f_q(x) = \sum_{i=1}^m (r_i^* - p_i^*) k(x_i, x) + b. \quad (19)$$

The asymptotical properties of the SSVQR model remain similar to the SVQR model detailed in (Takeuchi et al. (2006)).

4.2 PI estimation through SSVQR

We detail the algorithm for PI estimation through SSVQR in 2. The SSVQR PI preserves the properties of the SVQR PI, including the global optimal solution, PI tube movement, asymptotic guarantees, and distribution-free estimation, while also achieving a sparse solution.

Algorithm 2 PI estimation through SSVQR

```

1: procedure :- PI THROUGH SSVQR( $T, 1 - \alpha$ )
2:   Choose some  $\bar{q} \in (0, 1 - \alpha)$ 
3:   for each  $q \in \{\bar{q}, (1 + \bar{q} - \alpha)\}$  do
4:     Solve the LPP problem (18) by tuning the value of  $C$ . Obtain the solution  $(r^*, p^*, b^*)$ .
5:     Estimate the function  $f_q(x)$  using the (19).
6:   return  $(f_{\bar{q}}(x), f_{1+\bar{q}-\alpha}(x))$ 

```

4.3 Feature selection in PI estimation through SSVQR

Similar to other machine learning tasks, the PI estimation in high-dimensional settings also presents several challenges. The increased dimensionality not only increase the complexity of the PI bounds but also necessitates a larger sample size to ensure the quality of the estimate PI. Therefore, an efficient feature selection method is crucial for reducing the overall complexity of the PI estimation, particularly when dealing with high-dimensional data.

Algorithm 3 Feature selection through SSVQR

```

1: procedure :- FEATURE SELECTION THROUGH SSVQR( $T, 1 - \alpha, \epsilon$ )
2:   Choose some  $\bar{q} \in (0, 1 - \alpha)$ 
3:   for each  $q \in \{\bar{q}, (1 + \bar{q} - \alpha)\}$  do
4:     Consider the linear kernel  $k(x_i, x_j) = x_i^T x_j$  at the LPP (18).
5:     Solve the LPP (18) and obtain its solution  $(r^*, p^*, b^*)$ .
6:     Obtain the  $w_q$  using  $[x_1, x_2, \dots, x_m](r^* - p^*)$ .
7:     Compute  $I_{\bar{q}} = \{i : |w_{\bar{q}}(i)| \leq \epsilon\}$  and  $I_{1+\bar{q}-\alpha} = \{i : |w_{1+\bar{q}-\alpha}(i)| \leq \epsilon\}$ 
8:     Compute  $I = I_{\bar{q}} \cap I_{1+\bar{q}-\alpha}$  and Feature Set =  $\{1, 2, \dots, m\} - I$ 
9:   return (Feature Set)

```

We detail the feature selection algorithm through SSVQR model for the linear PI estimation task in Algorithm 3. Here, a linear PI refers to the PI, where both bounds are linear functions of the input variables ,i.e. $f_{\bar{q}}(x) = w_{\bar{q}}^T x + b_{\bar{q}}$ $f_{1+\bar{q}-\alpha}(x) = w_{1+\bar{q}-\alpha}^T x + b_{1+\bar{q}-\alpha}$.

The input of Algorithm 3 is the training set $T = \{(x_i, y_i), x_i \in \mathbf{R}^n, y_i \in \mathbf{R}, i = 1, 2, \dots, m\}$, specified confidence $(1 - \alpha)$, and a very small number ϵ . It finally returns the selected feature set. In the next section, we have explored several real-world datasets with numerous features and successfully perform feature selection using the SSVQR method for linear PI estimation, without compromising the quality of the estimated PI.

4.4 Conformal Regression in SVM

Finally, we extend the SVM models in CR setting for obtaining the finite sample test set guarantees. In split CR setting, we detail the SVM based CR algorithm as follows.

Compared to neural network (NN)-based CR models, the SVM-based CR model offers not only greater interpretability but also more stable prediction sets. In contrast, NN-based CR models often produce varying prediction set across different training runs, even when trained on the same data splits (I_1 and I_2) and with identical hyperparameter settings. It is because that unlike SVMs, NN models often converge to different local optima during training. We empirically verify these advantages of the SVM based CR model in next section.

Algorithm 4 CR through SVQR

```
1: procedure :- CR THROUGH SVQR( $T, 1 - \alpha$ )
2:   Split the training set  $T$  into  $I_1$  and calibration set  $I_2$ .
3:   Choose some  $\bar{q} \in (0, 1 - \alpha)$ 
4:   for each  $q \in \{\bar{q}, (1 + \bar{q} - \alpha)\}$  do
5:     Solve the QPP problem (4) on  $I_1$  by tuning the value of  $C$ . Obtain the solution  $(\alpha^*, \beta^*)$ .
6:     Estimate the function  $f_q(x)$  using the (5).
7:   Evaluate the nonconformity score  $E_i = \max\{f_{\bar{q}}(x) - y_i, y_i - f_{1-\bar{q}+\alpha}(x)\}$  on  $I_2$ .
8:   Compute the  $Q_{1-\alpha}(E, I_2) = (1 - \alpha)(1 + \frac{1}{|I_2|})$ -th empirical quantile of the non-conformity score  $E_i$ .
9:   return  $C(x_{m+1}) = [f_{\bar{q}}(x_{m+1}) - Q_{(1-\alpha)}(E, I_2), f_{1-\bar{q}+\alpha}(x_{m+1}) + Q_{1-\alpha}(E, I_2)]$ 
```

5 Experimental Results

In this section, we present the numerical results to analyze the quality of the PI obtained by the different SVM models through a series of experiments on simulated/artificial and real-world benchmark datasets. We also evaluate the effectiveness of the proposed SSVQR model and assess the quality of the PI estimated using it. We apply our Algorithm 3 for feature selection in high-dimensional real-world benchmark datasets for the linear PI estimation task. We have also compared the SVM based probabilistic forecasting models with the deep forecasting models on several time-series benchmark datasets.

One of the key strengths of SVM machines is their ability to always obtain the global optimal solution, maintaining their relevance and applicability in modern cutting-edge technology. As detailed in Table 1, PI estimation through SVQR and LS-SVR only obtains the global optimal solution but lacks the sparsity. In contrast, the proposed SSVQR PI can obtain the optimal global solution as well as the sparse solution. In view of this, we find the SVQR and LS-SVR model are qualified enough to be compared with the SSVQR model for the PI estimation task in SVM framework. The Tube and LUBE loss PI estimation methods available in SVM framework do not guarantee the global optimal solution and their solution may vary with the choice of initialization. However, we have considered the Tube loss and an improved version of the LUBE loss, the QD loss function (Pearce et al. (2018)) in deep forecasting models to compare their performance with the SVM based probabilistic forecasting models.

5.1 Evaluation Criteria and Parameter Tuning

Now, we describe in detail the evaluation criteria that will be used for our experiments. In all of our experiments, our aim is to estimate the PI with a confidence level of $1 - \alpha = 0.95$ that requires the estimation of the pair of quantile functions $(f_q(x), f_{q+0.95}(x))$, where $0 \leq q \leq 0.05$. In case of artificial datasets, we know the noise distribution and the true quantile function can be easily computed by the inverse of the cumulative distribution function. Therefore, the quality of the quantile function can be accurately assessed by computing the RMSE between the true and estimated quantile functions. In the absence of information about the noise distribution, the quality of the quantile function can be evaluated using Coverage Probability (CP), which measures the fraction of y values falling below the estimated quantile function. For a q^{th} quantile estimate, the CP should be as close as possible to q . For evaluating the overall quality of PI estimation, we use PICP and MPIW as assessment criteria. An effective PI method must achieve the target $1 - \alpha$ calibration while minimizing the PI width, as measured by the MPIW value. Furthermore, we define the Prediction Interval Coverage Error (PICE) as $\max(0, (1 - \alpha) - PICP)$ to quantify the extent to which the model falls short of the target calibration $(1 - \alpha)$. For comparing PI estimation models, a natural decision criterion is that the model with the lowest PICE should be considered the best. If all models successfully achieve the target calibration, the one with the minimum MPIW should be deemed the most optimal.

To estimate both bounds of the PI, we utilize the RBF kernel, defined as $k(x_i, x_j) = e^{-q\|x_i - x_j\|^2}$. As detailed in Algorithm 1 and Algorithm 2, SVQR and SSVQR require solving the QPP (4) and LPP (18) twice to obtain the quantile bounds of the PI respectively. We solve the QPPs of the SVQR PI model and the LPPs of the SSVQR model in MATLAB using the 'quadprog' and 'linprog' packages respectively. The SVQR

| | $(\bar{q}, 1 + \bar{q} - \alpha)$ | RMSE(Lw,Up) | Spar (Lw,Up) | CP (Lw,Up) | PICP | PICE | MPIW | Time (s) |
|-------|-----------------------------------|------------------|--------------|------------------|-------|------|--------|----------|
| SVQR | (0.01, 0.96) | (1.8021, 1.4446) | (0%, 0%) | (0.0110, 0.9680) | 0.957 | 0 | 2.9054 | 0.4783 |
| | (0.015, 0.965) | (1.7046, 1.4653) | (0%, 0%) | (0.0150, 0.9720) | 0.957 | 0 | 2.8244 | 0.5485 |
| | (0.02, 0.97) | (1.6519, 1.4799) | (0%, 0%) | (0.0180, 0.9720) | 0.954 | 0 | 2.7855 | 0.4712 |
| | (0.025, 0.975) | (1.5857, 1.5016) | (0%, 0%) | (0.0220, 0.9760) | 0.954 | 0 | 2.7379 | 0.4928 |
| | (0.03, 0.98) | (1.5030, 1.5667) | (0%, 0%) | (0.0250, 0.9800) | 0.955 | 0 | 2.7212 | 0.6054 |
| SSVQR | (0.01, 0.96) | (1.8060, 1.4418) | (15%, 18%) | (0.0110, 0.9680) | 0.957 | 0 | 2.9056 | 0.6157 |
| | (0.015, 0.965) | (1.7051, 1.4714) | (15%, 18%) | (0.0150, 0.9700) | 0.955 | 0 | 2.8275 | 0.5844 |
| | (0.02, 0.97) | (1.6497, 1.4861) | (15%, 18%) | 0.0160, 0.9720 | 0.956 | 0 | 2.7939 | 0.6169 |
| | (0.025, 0.975) | (1.5517, 1.4978) | (15%, 20%) | (0.0250, 0.9750) | 0.95 | 0 | 2.6995 | 0.5546 |
| | (0.03, 0.98) | (1.5133, 1.5604) | (16%, 20%) | (0.0290, 0.9800) | 0.951 | 0 | 2.7288 | 0.515 |

Table 2: Performance of the SVQR and SSVQR PI models on AD 1 dataset.

| | $(\bar{q}, 1 + \bar{q} - \alpha)$ | RMSE(Lw,Up) | Spar (Lw,Up) | CP (Lw,Up) | PICP | PICE | MPIW | Time (s) |
|-------|-----------------------------------|------------------|--------------|------------------|-------|-------|--------|----------|
| SVQR | (0.01, 0.96) | (4.2653, 5.7073) | (0%, 0%) | (0.0100, 0.9470) | 0.937 | 0.013 | 8.3755 | 0.805 |
| | (0.015, 0.965) | (4.1993, 6.0698) | (0%, 0%) | (0.0210, 0.9520) | 0.931 | 0.019 | 8.6865 | 0.699 |
| | (0.02, 0.97) | (4.1312, 6.5751) | (0%, 0%) | (0.0220, 0.9610) | 0.939 | 0.011 | 9.1619 | 0.6595 |
| | (0.025, 0.975) | (4.0525, 6.8163) | (0%, 0%) | (0.0340, 0.9650) | 0.931 | 0.019 | 9.3256 | 0.719 |
| | (0.03, 0.98) | (4.0251, 7.4745) | (0%, 0%) | (0.0350, 0.9720) | 0.937 | 0.013 | 9.978 | 0.6809 |
| SSVQR | (0.01, 0.96) | (4.1628, 5.5481) | (20%, 15%) | (0.0080, 0.9390) | 0.931 | 0.019 | 8.1036 | 0.502 |
| | (0.015, 0.965) | (4.0206, 5.9335) | (18%, 18%) | (0.0100, 0.9520) | 0.942 | 0.008 | 8.346 | 0.5173 |
| | (0.02, 0.97) | (4.0156, 6.3077) | (20%, 25%) | (0.0110, 0.9640) | 0.953 | 0 | 8.7801 | 0.5128 |
| | (0.025, 0.975) | (3.9444, 7.1596) | (15%, 20%) | (0.0240, 0.9680) | 0.944 | 0.006 | 9.5723 | 0.4694 |
| | (0.03, 0.98) | (3.9309, 7.3834) | (20%, 20%) | (0.0290, 0.9740) | 0.945 | 0.005 | 9.8075 | 0.5113 |

Table 3: Performance of the SVQR and SSVQR PI models on AD 2 dataset.

problem(4) or SSVQR (18) problem requires the supply of the two user defined parameters C and RBF kernel parameter q for non-linear PI estimation. We have tunned the value of the these parameters using the grid search in the search space $\{2^{-8}, 2^{-7}, \dots, 2^7, 2^8\} \times \{2^{-8}, 2^{-7}, \dots, 2^7, 2^8\}$.

5.2 Artificial Datasets

First, we generate six distinct artificial datasets. In each dataset, the values of x_i are randomly sampled from a uniform distribution $U(-5, 5)$, while the corresponding y_i values are obtained by polluting the function $(1 - x_i + 2x_i^2)e^{-0.5x_i^2}$ with different types of noise as described below.

$$\text{AD 1:- } y_i = (1 - x_i + 2x_i^2)e^{-0.5x_i^2} + \xi_i, \text{ where } \xi_i \sim N(0, 0.6)$$

$$\text{AD 2:- } y_i = (1 - x_i + 2x_i^2)e^{-0.5x_i^2} + \xi_i, \text{ where } \xi_i \sim \chi^2(3)$$

$$\text{AD 3:- } y_i = (1 - x_i + 2x_i^2)e^{-0.5x_i^2} + \xi_i, \text{ where } \xi_i \sim N(0, 0.4)$$

$$\text{AD 4:- } y_i = (1 - x_i + 2x_i^2)e^{-0.5x_i^2} + \xi_i, \text{ where } \xi_i \sim N(0, 0.8)$$

$$\text{AD 5:- } y_i = (1 - x_i + 2x_i^2)e^{-0.5x_i^2} + \xi_i, \text{ where } \xi_i \sim U(-5, 5)$$

$$\text{AD 6:- } y_i = (1 - x_i + 2x_i^2)e^{-0.5x_i^2} + \xi_i, \text{ where } \xi_i \sim U(-4, 4)$$

In case of each dataset, 2500 data points are generated in which 1000 data points are considered for training and rest of them are considered for testing.

5.3 Artificial Datasets Results, Discussion and Analysis

We present the performance of the SVQR and SSVQR model for PI estimation task with the different values of \bar{q} for each of simulated dataset in Table 2-7. The rightmost column of these Tables list the different pairs of target quantiles $(\bar{q}, 1 + \bar{q} - \alpha)$, required for the PI estimation with 0.95 confidence level. As detailed in Section 5.1 of this paper, for artificial datasets, the quality of the estimated upper and lower quantiles of the PI can be best evaluated by computing the RMSE between the estimated quantiles and their corresponding true quantile functions. The third column of the Tables 2-7 list these RMSE for different values of \bar{q} and mean of them are plotted at Figure 3 for lower and upper quantile estimation separately for different simulated

| | $(\bar{q}, 1 + \bar{q} - \alpha)$ | RMSE(Lw,Up) | Spar (Lw,Up) | CP (Lw,Up) | PICP | PICE | MPIW | Time (s) |
|-------|-----------------------------------|------------------|--------------|------------------|-------|-------|--------|----------|
| SVQR | (0.01, 0.96) | (1.7894, 1.5837) | (0%, 0%) | (0.0120, 0.9570) | 0.945 | 0 | 2.9 | 0.4872 |
| | (0.015, 0.965) | (1.7355, 1.6297) | (0%, 0%) | (0.0130, 0.9590) | 0.946 | 0.004 | 2.887 | 0.5077 |
| | (0.02, 0.97) | (1.5696, 1.6407) | (0%, 0%) | (0.0230, 0.9590) | 0.936 | 0.014 | 2.7223 | 0.5004 |
| | (0.025, 0.975) | (1.5070, 1.6927) | (0%, 0%) | (0.0280, 0.9680) | 0.94 | 0.01 | 2.71 | 0.4907 |
| | (0.03, 0.98) | (1.4694, 1.7477) | (0%, 0%) | (0.0300, 0.9750) | 0.945 | 0.005 | 2.7394 | 0.4745 |
| SSVQR | (0.01, 0.96) | 1.8411, 1.5781 | 20%, 40% | 0.0120, 0.9570 | 0.945 | 0.005 | 2.9462 | 0.4367 |
| | (0.015, 0.965) | (1.8297, 1.5917) | (40%, 30%) | (0.0120, 0.9570) | 0.945 | 0.005 | 2.9458 | 0.4563 |
| | (0.02, 0.97) | (1.6999, 1.6969) | (40%, 40%) | (0.0180, 0.9600) | 0.942 | 0.008 | 2.9026 | 0.4671 |
| | (0.025, 0.975) | (1.6509, 1.7191) | (40%, 40%) | (0.0220, 0.9620) | 0.94 | 0.01 | 2.8817 | 0.4501 |
| | (0.03, 0.98) | (1.4865, 1.7721) | (30%, 40%) | (0.0290, 0.9700) | 0.941 | 0.009 | 2.7739 | 0.4717 |

Table 4: Performance of the SVQR and SSVQR PI models on AD 3 dataset.

| | $(\bar{q}, 1 + \bar{q} - \alpha)$ | RMSE(Lw,Up) | Spar (Lw,Up) | CP (Lw,Up) | PICP | PICE | MPIW | Time (s) |
|-------|-----------------------------------|------------------|--------------|------------------|-------|-------|--------|----------|
| SVQR | (0.01, 0.96) | (2.5953, 2.1197) | (0%, 0%) | (0.0160, 0.9530) | 0.937 | 0.013 | 4.1549 | 0.723 |
| | (0.015, 0.965) | (2.5595, 2.1292) | (0%, 0%) | (0.0160, 0.9530) | 0.937 | 0.013 | 4.1268 | 0.6713 |
| | (0.02, 0.97) | (2.4221, 2.2193) | (0%, 0%) | (0.0200, 0.9610) | 0.941 | 0.009 | 4.0817 | 0.6704 |
| | (0.025, 0.975) | (2.2561, 2.2555) | (0%, 0%) | (0.0290, 0.9630) | 0.934 | 0.016 | 3.9365 | 0.6815 |
| | (0.03, 0.98) | (2.2211, 2.3699) | (0%, 0%) | (0.0310, 0.9670) | 0.936 | 0.014 | 4.0273 | 0.6343 |
| SSVQR | (0.01, 0.96) | (2.5842, 2.1364) | (20%, 40%) | (0.0160, 0.9530) | 0.937 | 0.013 | 4.1577 | 0.4704 |
| | (0.015, 0.965) | (2.5475, 2.1911) | (20%, 20%) | (0.0160, 0.9560) | 0.94 | 0.01 | 4.1802 | 0.4745 |
| | (0.02, 0.97) | (2.4939, 2.2455) | (20%, 20%) | (0.0190, 0.9610) | 0.942 | 0.008 | 4.183 | 0.4818 |
| | (0.025, 0.975) | (2.3617, 2.3037) | (40%, 20%) | (0.0240, 0.9640) | 0.94 | 0.01 | 4.1002 | 0.4662 |
| | (0.03, 0.98) | (2.2689, 2.4147) | (40%, 20%) | (0.0290, 0.9700) | 0.941 | 0.009 | 4.121 | 0.4884 |

Table 5: Performance of the SVQR and SSVQR PI models on AD 4 dataset.

| | $(\bar{q}, 1 + \bar{q} - \alpha)$ | RMSE(Lw,Up) | Spar (Lw,Up) | CP (Lw,Up) | PICP | PICE | MPIW | Time (s) |
|-------|-----------------------------------|------------------|--------------|------------------|-------|-------|--------|----------|
| SVQR | (0.01, 0.96) | (4.9694, 4.4016) | (0%, 0%) | (0.0100, 0.9560) | 0.946 | 0.004 | 8.1044 | 0.7917 |
| | (0.015, 0.965) | (4.8456, 4.4539) | (0%, 0%) | (0.0180, 0.9600) | 0.942 | 0.008 | 8.0257 | 0.8009 |
| | (0.02, 0.97) | (4.8100, 4.4860) | (0%, 0%) | (0.0190, 0.9620) | 0.943 | 0.007 | 8.0223 | 0.736 |
| | (0.025, 0.975) | (4.7111, 4.5143) | (0%, 0%) | (0.0280, 0.9640) | 0.936 | 0.014 | 7.943 | 0.6895 |
| | (0.03, 0.98) | (4.6921, 4.5368) | (0%, 0%) | (0.0290, 0.9680) | 0.939 | 0.011 | 7.9481 | 0.6191 |
| SSVQR | (0.01, 0.96) | (5.2658, 4.5044) | (40%, 30%) | (0.0050, 0.9610) | 0.956 | 0 | 8.5344 | 0.5394 |
| | (0.015, 0.965) | (4.8787, 4.5073) | (35%, 30%) | (0.0160, 0.9610) | 0.945 | 0.005 | 8.1171 | 0.4835 |
| | (0.02, 0.97) | (4.8138, 4.5249) | (30%, 30%) | (0.0190, 0.9650) | 0.946 | 0.004 | 8.0659 | 0.472 |
| | (0.025, 0.975) | (4.7464, 4.6037) | (25%, 30%) | (0.0260, 0.9670) | 0.941 | 0.009 | 8.0692 | 0.5102 |
| | (0.03, 0.98) | (4.6962, 4.7637) | (30%, 40%) | (0.0290, 0.9720) | 0.943 | 0.007 | 8.1832 | 0.5068 |

Table 6: Performance of the SVQR and SSVQR PI models on AD 5 dataset.

| | $(\bar{q}, 1 + \bar{q} - \alpha)$ | RMSE(Lw,Up) | Spar (Lw,Up) | CP (Lw,Up) | PICP | PICE | MPIW | Time (s) |
|-------|-----------------------------------|------------------|--------------|------------------|-------|-------|---------|----------|
| SVQR | (0.01, 0.96) | (6.1510, 5.5057) | (0%, 0%) | (0.0110, 0.9630) | 0.952 | 0 | 10.0826 | 0.6437 |
| | (0.015, 0.965) | (6.0517, 5.5584) | (0%, 0%) | (0.0150, 0.9670) | 0.952 | 0 | 10.031 | 0.6798 |
| | (0.02, 0.97) | (5.9777, 5.6130) | (0%, 0%) | (0.0170, 0.9700) | 0.953 | 0 | 10.0141 | 1.0752 |
| | (0.025, 0.975) | (5.8879, 5.6868) | (0%, 0%) | (0.0230, 0.9760) | 0.953 | 0 | 9.9987 | 0.9265 |
| | (0.03, 0.98) | (5.7599, 5.7156) | (0%, 0%) | (0.0290, 0.9780) | 0.949 | 0.001 | 9.8878 | 0.9445 |
| SSVQR | (0.01, 0.96) | (5.9304, 5.4581) | (10%, 15%) | (0.0110, 0.9610) | 0.95 | 0 | 9.7944 | 0.569 |
| | (0.015, 0.965) | (5.9107, 5.5686) | (10%, 20%) | (0.0140, 0.9700) | 0.956 | 0 | 9.9016 | 0.5656 |
| | (0.02, 0.97) | (5.7836, 5.5880) | (15%, 25%) | (0.0180, 0.9700) | 0.952 | 0 | 9.7807 | 0.5766 |
| | (0.025, 0.975) | (5.6486, 5.6038) | (20%, 20%) | (0.0260, 0.9710) | 0.945 | 0.005 | 9.6443 | 0.5423 |
| | (0.03, 0.98) | (5.6184, 5.6506) | (10%, 15%) | (0.0300, 0.9760) | 0.946 | 0.004 | 9.6653 | 0.5636 |

Table 7: Performance of the SVQR and SSVQR PI models on AD 6 dataset.



Figure 3: Comparison of the quality of quantile function obtained by the SVQR and SSVQR PI models.

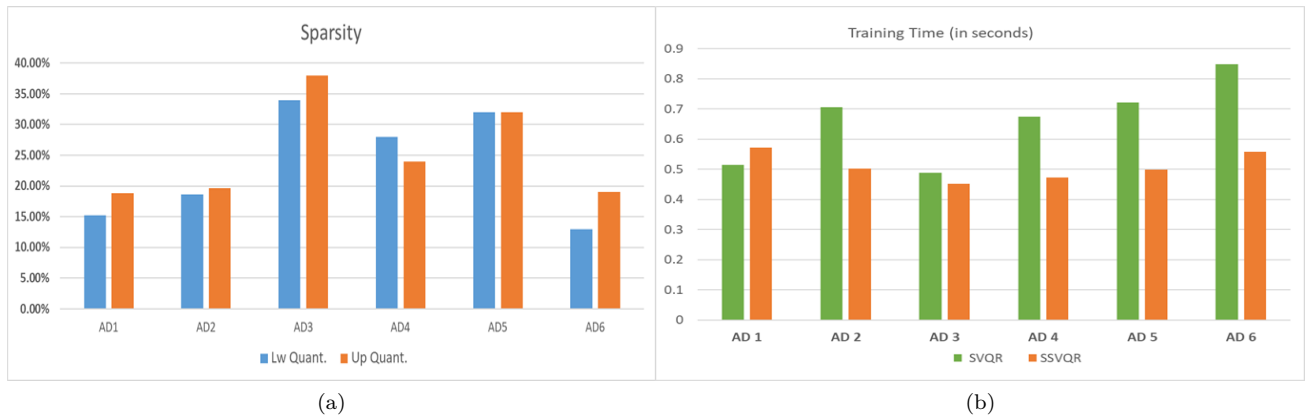


Figure 4: (a) Quantile functions estimated by the proposed SSVQR model is sparse while SVQR model fails to obtain the sparse solution. (b) Average training time comparison of the SVQR and SSVQR models for PI estimation.

datasets. The quantile bounds estimated by the SSVQR model are comparable to, or slightly better than, those obtained from the SVQR model. Replacing L_2 regularization with L_1 regularization in the SVM quantile regression model does not result in significantly different estimates. However, the major advantage of using the SSVQR model is its ability to obtain the sparse solution vector. Figure 4(a) plots the sparsity of the solution vector corresponding to the upper and lower quantile bounds obtained by the SSVQR model. It highlights that the SSVQR model effectively reduces significant coefficients of the solution vector to near zero which enables the feature selection task in PI estimation and also simplify the overall prediction process.

We compare the overall average training time (in seconds) taken by the SVQR PI and SSVQR PI models for the PI estimation task across different artificial datasets in Figure 4(b). It shows that the SSVQR requires fewer seconds to train the PI model than the SVQR model. We have solved the QPPs of the SVQR PI model and LPPs of the SSVQR model in MATLAB with 'quadprog' and 'linprog' packages respectively.

Another key observation from the numerical results in Tables 2-7 is the consistent performance of the SVQR and SSVQR PI models across different datasets. In all cases, both the SVQR and SSVQR PI models manage to approximately achieve 95% target coverage. We plot the MPIW values obtained by the SSVQR and SVQR PI models against different values of \bar{q} on dataset AD2 and AD4 in Figure 5. On AD2 dataset, the MPIW values of the PI obtained by both models increase with \bar{q} . It is evident from Table 3 that this increase is

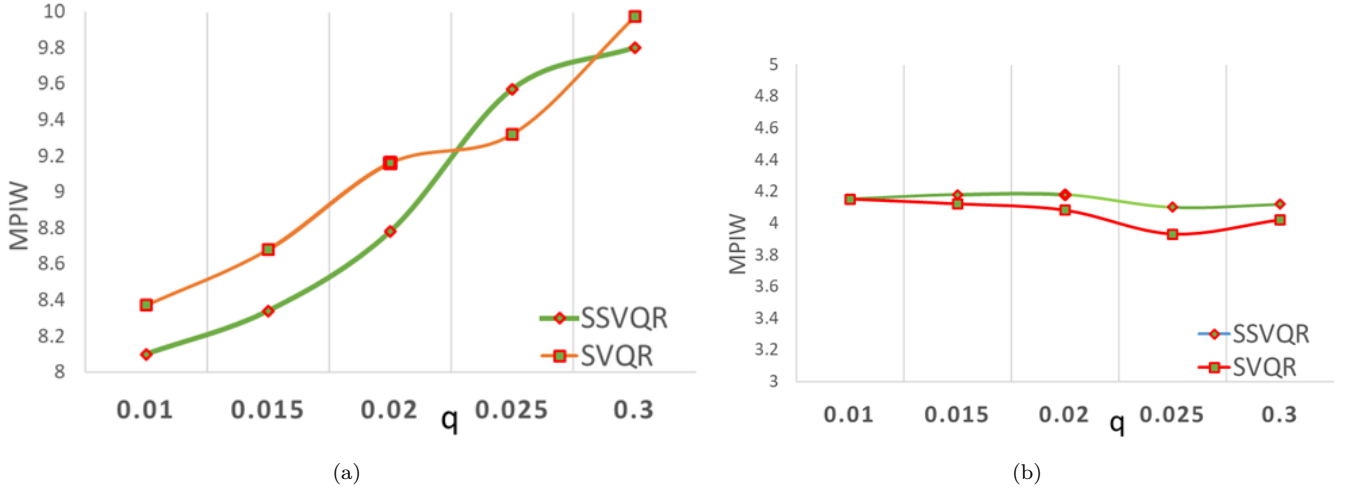


Figure 5: Plot of the MPIW obtained by the SVQR and SSVQR PI models against \bar{q} on (a) AD2 and (b) AD4 dataset.

not related to the PICP values obtained by the SVQR and SSVQR PI models. Actually, it is caused by the nature of noise present in the AD2 dataset. The AD2 dataset contains asymmetric noise from the (χ^2) distribution, leading to a higher density of data points in the lower region of the input-target space, which gradually decreases as we move upward. As \bar{q} decreases, the resultant PI shifts downward, passing through denser regions of the data cloud, leading to lower MPIW values. It shows that the movement of the PI tube due to change of \bar{q} values may lead to the narrower PI particularly in presence of the asymmetric noise in the data. Apart from the AD2 dataset, all other artificial datasets contain noise from symmetric distributions. In these datasets, the centered PI $((f_{0.025}(x), f_{0.975}(x)))$ is expected to achieve the high quality PI. Figure 5(b) shows that at $q = 0.025$, both the SVQR and SSVQR PI models attain the lowest MPIW values on AD4 dataset.

5.4 Feature Selection through SSVQR

Next, we apply our SSVQR model for feature selection in PI estimation with linear kernel. To demonstrate this, we use five popular real-world benchmark datasets namely Spambase, Student Performance, Boston Housing, UCI-secom and MADELON. We use the 80% of data points for training and use rest of them for testing. We set the target calibration $1 - \alpha = 0.95$. Following Algorithm 3, we perform feature selection using the SSVQR PI model for $\bar{q} = 0.025$ and present the results in Table 8. The numerical results clearly demonstrate that the SSVQR PI feature selection (as detailed in Algorithm 3) can significantly reduce the number of features while maintaining the quality of the PI, as measured by PICP and MPIW. On average, it could reduce the 69% of features on considered datasets and reduce the complexity of the PI estimation task significantly. The training time of the PI estimating task improves significantly after dropping irrelevant features through Algorithm 3. On average, it could improve the 53% improvement in training time. Also, reducing the significant numbers of features will reduce the tuning and testing time of the PI model.

For high-dimensional datasets such as UCI secom and MADELON, feature selection leads to a significant improvement in the quality of the estimated PI in terms of its coverage. The SSVQR based feature selection algorithm eliminates a significant number of irrelevant features and learn the PI in relatively much lower dimension which results in better PI coverage with linear functions. Table 9 lists the features dropped by the SSVQR-PI feature selection algorithm for each dataset.

5.5 SVM PI estimation methods on benchmark datasets

We have done experiments on the two popular benchmark datasets namely Boston Housing and Concrete and evaluate the quality of the PI estimated by the SSVQR, SVQR and LS-SVR based PI estimation methods for

| Dataset | Dimension | Before Feature Selection | | | After Feature Selection | | | % Reduced Features |
|----------------|-------------|--------------------------|---------|---------------|-------------------------|---------|---------------|-----------------------|
| | | PICP | MPIW | Train Time(s) | PICP | MPIW | Train Time(s) | |
| Spambase | (4601, 58) | 0.9663 | 0.9330 | 60 | 0.9653 | 0.9340 | 52 | 46% |
| Student Perf. | (395, 16) | 0.8861 | 6.8429 | 0.48 | 0.8861 | 6.8429 | 0.42 | 73% |
| Boston Housing | (505, 14) | 0.9406 | 23.0647 | 0.81 | 0.9406 | 23.0647 | 0.7 | 38% |
| uci-secom | (1568, 591) | 0.8758 | 1.6146 | 16 | 0.9204 | 1.6683 | 7 | 91% |
| MADOLON | (2000, 500) | 0.7100 | 2.0007 | 58 | 0.9375 | 2.0020 | 11 | 99% |

Table 8: Performance comparison before and after feature selection using the SSVQR PI model

| Dataset | Dropped Features |
|----------------|---|
| Spambase | 2, 8, 11, 13, 16, 17, 18, 19, 20, 21, 22, 23, 25, 27, 31, 35, 37, 46, 47, 48, 49, 50, 53, 54, 55, 56 |
| Student Perf. | 1, 2, 3, 4, 5, 6, 7, 8, 9, 10, 11 |
| Boston Housing | 2, 3, 4, 7, 10 |
| UCI Secom | 1, 4-20, 22-27, 28-41, 42-50, 52-58, 60-66, 68-70, 72, 74-87, 89, 91-110, 112-132, 134, 137-138, 140-157, 159-160, 162-187, 189-203, 205-224, 226-246, 247-296, 297-332, 333-362, 364-386, 387-400, 401-418, 420-422, 424-431, 434-435, 437-438, 440-466, 467, 469-481, 483, 489-498, 501-509, 512-520, 522-538, 540-545, 546, 548-560, 563-569, 571, 573-579, 580, 582-587 |
| MADOLON | 0-89, 91-227, 229-275, 277-331, 333-444, 446-499 |

Table 9: Feature Selection by SSVQR PI

different value of the \bar{q} with non-linear RBF kernel. Table 10 and 11 contains the numerical results obtained on the Boston Housing and Concrete datasets respectively. We can observe that the SSVQR, SVQR and LS-SVR PI models obtains a similar quality of the PI but SSVQR models always obtain the sparse solution vector.

| | q | Spar (Lw, Up) | CP (Lw, Up) | PICP | PICE | MPIW | Time (s) |
|--------|----------------|---------------|----------------|------|------|-------|----------|
| SVQR | (0.025, 0.925) | (0%, 0%) | (0.028, 0.930) | 0.90 | 0 | 28.55 | 0.1347 |
| | (0.05, 0.95) | (0%, 0%) | (0.052, 0.950) | 0.90 | 0.00 | 33.06 | 0.1472 |
| | (0.075, 0.975) | (0%, 0%) | (0.088, 0.972) | 0.88 | 0.02 | 38.23 | 0.1670 |
| SSVQR | (0.025, 0.925) | (17%, 16%) | (0.027, 0.927) | 0.90 | 0 | 28.62 | 0.0657 |
| | (0.05, 0.95) | (15%, 22%) | (0.048, 0.947) | 0.90 | 0 | 32.77 | 0.0678 |
| | (0.075, 0.975) | (14%, 28%) | (0.080, 0.967) | 0.89 | 0.01 | 38.24 | 0.0681 |
| LS-SVR | (0.025, 0.925) | (0%, 0%) | | 0.91 | 0 | 31.19 | 0.0064 |
| | (0.050, 0.950) | (0%, 0%) | | 0.91 | 0 | 30.18 | 0.0067 |
| | (0.075, 0.975) | (0%, 0%) | | 0.89 | 0.01 | 31.19 | 0.0060 |

Table 10: Comparison of different SVM PI estimation methods on Boston Housing

5.6 Probabilistic Forecasting with SVM models

In this section, we compare the performance of the proposed SSVQR, SVQR and LS-SVR model for the probabilistic forecasting. We also train several recent and widely adopted deep learning models for probabilistic forecasting developed in a distribution-free setting, including Quantile-based LSTM, Tube Loss LSTM, and Quality-Driven (QD) Loss LSTM models Pearce et al. (2018) to compare their performance against the SVM-based models. The QD loss Pearce et al. (2018) is the improved version of the LUBE model which can be used minimized with the gradient descent method in deep learning architecture. Also, we have added the popular Deep AR (Salinas et al. (2020)) probabilistic forecasting method for baseline comparison.

We consider three popular time-series datasets namely Female Births (365×1), Minimum Temperature (3651×1) and Beer Production (464×1). We have used the 70% of dataset as training set and rest of them are used for testing. Out of the training set, the last 10% of the observations have been used for the validation set. We present the numerical results in Table 12. All of the models were asked to obtain the probabilistic forecast for target calibration $1 - \alpha = 0.95$.

One major observation from the Table 12 is that the SVM based probabilistic forecasting models obtain competitive performance compared to complex LSTM based deep forecasting models after efficient tuning

| | q | Spar (Lw, Up) | CP (Lw, Up) | PICP | PICE | MPIW | Time (s) |
|--------|----------------|---------------|------------------|--------|--------|---------|----------|
| SVQR | (0.025, 0.925) | (0%, 0%) | (0.0219, 0.8997) | 0.8777 | 0.0723 | 32.5492 | 2.6141 |
| | (0.05, 0.95) | (0%, 0%) | (0.0408, 0.9436) | 0.9028 | 0.0472 | 28.6541 | 2.8405 |
| | (0.075, 0.975) | (0%, 0%) | (0.0690, 0.9561) | 0.8871 | 0.0629 | 32.1635 | 2.5197 |
| SSVQR | (0.025, 0.925) | (12%, 12%) | (0.0340, 0.9029) | 0.8689 | 0.0811 | 29.4962 | 0.1858 |
| | (0.05, 0.95) | (12%, 12%) | (0.0583, 0.9272) | 0.8689 | 0.0811 | 27.8917 | 0.1795 |
| | (0.075, 0.975) | 12%, 12% | (0.0777, 0.9515) | 0.8738 | 0.0762 | 30.2547 | 0.1837 |
| LS-SVR | (0.025, 0.925) | 0%,0% | | 0.9126 | 0.0374 | 28.2429 | 0.4125 |
| | (0.050, 0.950) | (0%,0%) | | 0.8932 | 0.0568 | 27.3308 | 0.4631 |
| | (0.075, 0.975) | (0%,0%) | | 0.9029 | 0.0471 | 28.2429 | 0.3954 |

Table 11: Comparison of different SVM PI estimation methods on Concrete dataset

of its parameters. Also, the SSVQR based probabilistic forecasting model obtains the sparse solution. Table 13 presents the tuned neural architectures of the LSTM models, along with the number of weights to be optimized for each of the probabilistic forecasting models used. The LSTM based probabilistic forecasting models are more complex and requires the optimization of thousands of weights where as the SVQR based probabilistic models are much simpler architectures and could obtain similar quality of the PI as obtained by the LSTM based models. Figure (6) (a) and (b) shows the forecasting of the SSVQR and SVQR model on Temperature and Beer Production datasets respectively.

| Dataset | Method | PICP | MPIW | Training Time | Sparsity |
|---------------|---------------|------|--------|---------------|----------|
| Female Births | SSVQR | 0.93 | 28.00 | 1.12 | 61 % |
| | SVQR | 0.95 | 27.11 | 0.97 | 0 % |
| | LS-SVR | 0.95 | 37.70 | 3.60 | 0 % |
| | Quantile LSTM | 0.95 | 28.20 | 118.00 | — |
| | Tube LSTM | 0.96 | 28.09 | 43.00 | — |
| | QD LSTM | 0.94 | 38.98 | — | — |
| | DeepAR | 0.94 | 29.8 | 55.0 | 0 % |
| Minimum Temp. | SSVQR | 0.96 | 10.72 | 200.79 | 69 % |
| | SVQR | 0.96 | 75.81 | 172.00 | 0 % |
| | LS-SVR | 0.95 | 10.59 | 0.53 | 0 % |
| | Quantile LSTM | 0.95 | 24.82 | 1135.00 | — |
| | Tube LSTM | 0.94 | 15.56 | 447.00 | — |
| | QD LSTM | 0.79 | 5.94 | — | — |
| | DeepAR | 0.90 | 12.79 | 58.0 | 0 % |
| Beer Prod. | SSVQR | 0.96 | 0.94 | 1.77 | 70 % |
| | SVQR | 0.95 | 75.73 | 0.78 | 0 % |
| | LS-SVR | 0.96 | 79.48 | 0.29 | 0 % |
| | Quantile LSTM | 0.94 | 134.80 | 132.80 | — |
| | Tube LSTM | 0.95 | 42.91 | 89.60 | — |
| | QD LSTM | 0.96 | 159.71 | — | — |
| | DeepAR | 0.76 | 12.43 | 62.0 | 0 % |

Table 12: Performance comparison of SVM and deep learning based probabilistic forecasting methods on benchmark datasets.

5.7 Numerical Results of SVM based Conformal Regression method

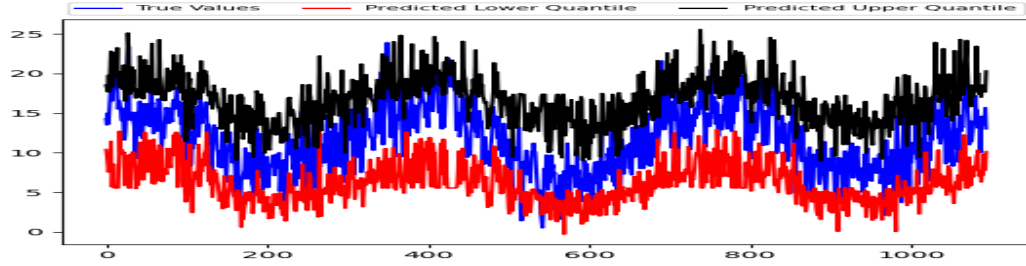
We now evaluate the performance of the SVM-based CR model (SVQR+CR) against the NN-based CQR model (CQR-NN) (Romano et al. (2019)) on several benchmark datasets under the split conformal setting, with the target coverage level $1 - \alpha = 0.90$. Both models were trained across 10 independent runs using fixed hyperparameter settings and identical splits of training and calibration sets.

The numerical results in Table 14 yield several insights. First, SVQR+CR achieved the target coverage in 4 out of 5 datasets, while CQR-NN did so in only 3 out of 5. Moreover, SVQR+CR yielded lower MPIW in 4 out of 5 cases.

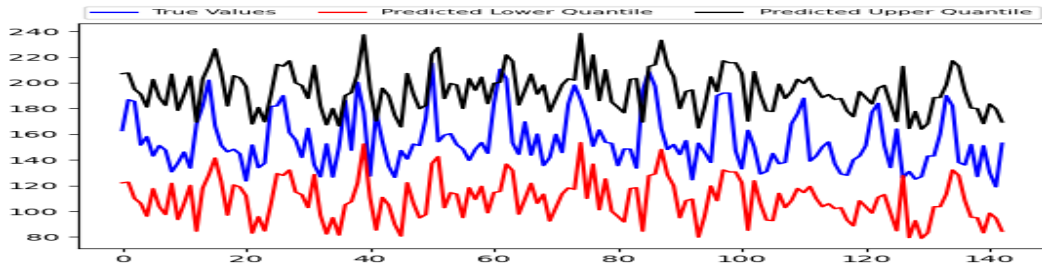
Most notably, the standard deviations of PICP and MPIW across the 10 runs were zero for SVQR+CR, indicating perfectly stable predictions. In contrast, CQR-NN exhibited significant fluctuations. This is because, due to the non-convex nature of their optimization landscape, NN models often converge to different

| Dataset | Model | Architecture | Weights | W. Size |
|---------------|---------------|--------------|---------|---------|
| Female Births | SVQR | Kernel | 256 | 10 |
| | SSVQR | Kernel | 256 | 15 |
| | LS-SVR | Kernel | 256 | 20 |
| | Quantile LSTM | LSTM [100] | 30 K | 25 |
| | Tube LSTM | LSTM [100] | 30 K | 25 |
| | QD LSTM | LSTM [100] | 30 K | 25 |
| Minimum Temp. | DeepAR | LSTM [40,40] | 13 K | 28 |
| | SVQR | Kernel | 2 556 | 12 |
| | SSVQR | Kernel | 2 556 | 18 |
| | LS-SVR | Kernel | 2 556 | 22 |
| | Quantile LSTM | LSTM [16,8] | 32 K | 28 |
| | Tube LSTM | LSTM [16,8] | 32 K | 28 |
| Beer Prod. | QD LSTM | LSTM [16,8] | 32 K | 28 |
| | DeepAR | LSTM [40,40] | 13 K | 56 |
| | SVQR | Kernel | 325 | 8 |
| | SSVQR | Kernel | 325 | 14 |
| | LS-SVR | Kernel | 325 | 18 |
| | Quantile LSTM | LSTM [64,32] | 29 K | 24 |
| | Tube LSTM | LSTM [64,32] | 29 K | 24 |
| | QD LSTM | LSTM [64,32] | 29 K | 24 |
| | DeepAR | LSTM [40,40] | 13 K | 48 |

Table 13: Comparison of the complexity of used SVM and deep learning based probabilistic forecasting models on benchmark datasets. LSTM [16,8] means that the used LSTM model has two hidden layer containing 16 and 8 neurons respectively.



(a)



(b)

Figure 6: Probabilistic forecasting with SSVQR model on daily (a) Temperature and (b) Beer Production dataset

local minima across different training trials, even when the training data and hyperparameter settings remain fixed. Another key advantage of SVQR+CR is its reduced training time compared to CQR-NN, making it a more efficient and stable choice for conformal regression task.

| Dataset | Method | Performance | | | Std. Dev. (CQR-NN) | | |
|----------|---------|-------------|-------|----------|--------------------|--------|----------|
| | | PICP (%) | MPIW | Time (s) | PICP | MPIW | Time (s) |
| Boston | CQR-NN | 94.12 | 2.19 | 2.65 | (1.14) | (0.12) | (0.23) |
| | SVQR+CP | 95.10 | 2.24 | 0.44 | (0.00) | (0.00) | (0.03) |
| Energy | CQR-NN | 87.66 | 1.13 | 3.20 | (1.12) | (0.03) | (0.31) |
| | SVQR+CP | 88.96 | 1.05 | 0.95 | (0.00) | (0.00) | (0.05) |
| Concrete | CQR-NN | 92.58 | 19.62 | 1.89 | (1.02) | (0.71) | (0.17) |
| | SVQR+CP | 91.35 | 18.74 | 0.38 | (0.00) | (0.00) | (0.01) |
| Yacht | CQR-NN | 91.69 | 2.43 | 1.44 | (1.49) | (0.35) | (0.12) |
| | SVQR+CP | 90.82 | 2.87 | 0.22 | (0.00) | (0.00) | (0.01) |
| Servo | CQR-NN | 88.39 | 0.73 | 1.15 | (2.21) | (0.10) | (0.09) |
| | SVQR+CP | 89.74 | 0.68 | 0.16 | (0.00) | (0.00) | (0.01) |

Table 14: Comprehensive comparison of CQR-NN and SVQR+CP.

6 Future Work

This paper presents a comprehensive roadmap for exploring UQ methods within the SVM regression framework. In contrast to NN models, SVM solutions exhibit lower uncertainty due to their tendency to converge to globally optimal solutions.

We proposed a feature selection algorithm tailored for PI estimation under the assumption that the bounds are linear functions of the input features. However, extending this approach to handle non-linear dependencies remains an important direction for future work, particularly in both NN and SVM-based models. Additionally, we show that SVM-based probabilistic forecasting models offer a compelling alternative to complex deep learning architectures by significantly reducing model complexity through the optimization of fewer parameters on batch datasets. Despite these advantages, they are not well-suited for dynamic or online data scenarios. To address this limitation, developing incremental or online SVM-based probabilistic forecasting models presents a promising avenue for future research. In this work, we have focused exclusively on the SVM regression model, a similar UQ analysis can be extended to SVM classification models in future research.

Acknowledgments

I shall be thankful to Shayam Saktawat, Nikhil Bhanose and Chaitanya Dahale for helping in experiments.

References

- Pritam Anand, Reshma Rastogi, and Suresh Chandra. A new asymmetric ϵ -insensitive pinball loss function based support vector quantile regression model. *Applied Soft Computing*, 94:106473, 2020.
- Pritam Anand, Tathagata Bandyopadhyay, and Suresh Chandra. Tube loss: A novel approach for prediction interval estimation and probabilistic forecasting. *arXiv preprint arXiv:2412.06853*, 2024.
- Christopher M Bishop. Mixture density networks. *Neural Computing & Applications*, 1994.
- Christopher M Bishop. Neural networks for pattern recognition. *Clarendon Press google schola*, 2:223–228, 1995.
- Alex J Cannon. Quantile regression neural networks: Implementation in r and application to precipitation downscaling. *Computers & geosciences*, 37(9):1277–1284, 2011.
- Qiang Cheng, Jale Tezcan, and Jie Cheng. Confidence and prediction intervals for semiparametric mixed-effect least squares support vector machine. *Pattern Recognition Letters*, 40:88–95, 2014.
- Kris De Brabanter, Jos De Brabanter, Johan AK Suykens, and Bart De Moor. Approximate confidence and prediction intervals for least squares support vector regression. *IEEE Transactions on Neural Networks*, 22(1):110–120, 2010.

-
- Richard D De VIEAUX, Jennifer Schumi, Jason Schweinsberg, and Lyle H Ungar. Prediction intervals for neural networks via nonlinear regression. *Technometrics*, 40(4):273–282, 1998.
- Yaoyao He, Yang Qin, Shuo Wang, Xu Wang, and Chao Wang. Electricity consumption probability density forecasting method based on lasso-quantile regression neural network. *Applied energy*, 233:565–575, 2019.
- JT Gene Hwang and A Adam Ding. Prediction intervals for artificial neural networks. *Journal of the American Statistical Association*, 92(438):748–757, 1997.
- James Kennedy and Russell Eberhart. Particle swarm optimization. In *Proceedings of ICNN’95-international conference on neural networks*, volume 4, pp. 1942–1948. iee, 1995.
- Abbas Khosravi, Saeid Nahavandi, Doug Creighton, and Amir F Atiya. Lower upper bound estimation method for construction of neural network-based prediction intervals. *IEEE transactions on neural networks*, 22(3):337–346, 2010.
- Roger Koenker and Gilbert Bassett Jr. Regression quantiles. *Econometrica: journal of the Econometric Society*, pp. 33–50, 1978.
- Philippe Lauret, Mathieu David, and Hugo TC Pedro. Probabilistic solar forecasting using quantile regression models. *energies*, 10(10):1591, 2017.
- David JC MacKay. The evidence framework applied to classification networks. *Neural computation*, 4(5):720–736, 1992.
- James Mercer. Xvi. functions of positive and negative type, and their connection the theory of integral equations. *Philosophical transactions of the royal society of London. Series A, containing papers of a mathematical or physical character*, 209(441-458):415–446, 1909.
- David A Nix and Andreas S Weigend. Estimating the mean and variance of the target probability distribution. In *Proceedings of 1994 ieee international conference on neural networks (ICNN’94)*, volume 1, pp. 55–60. IEEE, 1994.
- Harris Papadopoulos. Inductive conformal prediction: Theory and application to neural networks. In *Tools in artificial intelligence*. Citeseer, 2008.
- Harris Papadopoulos, Kostas Proedrou, Volodya Vovk, and Alex Gammerman. Inductive confidence machines for regression. In *Machine learning: ECML 2002: 13th European conference on machine learning Helsinki, Finland, August 19–23, 2002 proceedings 13*, pp. 345–356. Springer, 2002.
- Olivier C Pasche and Sebastian Engelke. Neural networks for extreme quantile regression with an application to forecasting of flood risk. *The Annals of Applied Statistics*, 18(4):2818–2839, 2024.
- Tim Pearce, Alexandra Brintrup, Mohamed Zaki, and Andy Neely. High-quality prediction intervals for deep learning: A distribution-free, ensembled approach. In *International conference on machine learning*, pp. 4075–4084. PMLR, 2018.
- Reshma Rastogi, Aman Pal, and Suresh Chandra. Generalized pinball loss svms. *Neurocomputing*, 322:151–165, 2018.
- Yaniv Romano, Evan Patterson, and Emmanuel Candes. Conformalized quantile regression. *Advances in neural information processing systems*, 32, 2019.
- David Salinas, Valentin Flunkert, Jan Gasthaus, and Tim Januschowski. Deepar: Probabilistic forecasting with autoregressive recurrent networks. *International journal of forecasting*, 36(3):1181–1191, 2020.
- Bernhard Schölkopf, Ralf Herbrich, and Alex J Smola. A generalized representer theorem. In *International conference on computational learning theory*, pp. 416–426. Springer, 2001.
- George Seber and George AF Seber. Nonlinear regression models. *The Linear Model and Hypothesis: A General Unifying Theory*, pp. 117–128, 2015.

-
- Nitin Anand Shrivastava, Abbas Khosravi, and Bijaya Ketan Panigrahi. Prediction interval estimation for electricity price and demand using support vector machines. In *2014 International Joint Conference on Neural Networks (IJCNN)*, pp. 3995–4002. IEEE, 2014.
- Nitin Anand Shrivastava, Abbas Khosravi, and Bijaya Ketan Panigrahi. Prediction interval estimation of electricity prices using pso-tuned support vector machines. *IEEE Transactions on Industrial Informatics*, 11(2):322–331, 2015.
- Johan AK Suykens, Jos De Brabanter, Lukas Lukas, and Joos Vandewalle. Weighted least squares support vector machines: robustness and sparse approximation. *Neurocomputing*, 48(1-4):85–105, 2002.
- Ichiro Takeuchi, Quoc V Le, Timothy D Sears, Alexander J Smola, and Chris Williams. Nonparametric quantile estimation. *Journal of machine learning research*, 7(7), 2006.
- Mohammad Tanveer, Sweta Sharma, Reshma Rastogi, and Pritam Anand. Sparse support vector machine with pinball loss. *Transactions on Emerging Telecommunications Technologies*, 32(2):e3820, 2021.
- James W Taylor. A quantile regression neural network approach to estimating the conditional density of multiperiod returns. *Journal of forecasting*, 19(4):299–311, 2000.
- Vladimir Vapnik. *The nature of statistical learning theory*. Springer science & business media, 2013.
- Vladimir Vovk, Alexander Gammerman, and Glenn Shafer. *Algorithmic learning in a random world*, volume 29. Springer, 2005.
- Volodya Vovk, Alexander Gammerman, and Craig Saunders. Machine-learning applications of algorithmic randomness. 1999.
- Can Wan, Jin Lin, Jianhui Wang, Yonghua Song, and Zhao Yang Dong. Direct quantile regression for nonparametric probabilistic forecasting of wind power generation. *IEEE Transactions on Power Systems*, 32(4):2767–2778, 2016.
- Ya-Fen Ye, Jie Wang, and Wei-Jie Chen. Nonlinear feature selection for support vector quantile regression. *Neural Networks*, 185:107136, 2025.
- Hao Zhang, Yongqian Liu, Jie Yan, Shuang Han, Li Li, and Quan Long. Improved deep mixture density network for regional wind power probabilistic forecasting. *IEEE Transactions on Power Systems*, 35(4):2549–2560, 2020a.
- Wenjie Zhang, Hao Quan, and Dipti Srinivasan. An improved quantile regression neural network for probabilistic load forecasting. *IEEE Transactions on Smart Grid*, 10(4):4425–4434, 2018.
- Wenjie Zhang, Hao Quan, Oktoviano Gandhi, Ram Rajagopal, Chin-Woo Tan, and Dipti Srinivasan. Improving probabilistic load forecasting using quantile regression nn with skip connections. *IEEE Transactions on Smart Grid*, 11(6):5442–5450, 2020b.